Hindawi
Advances in High Energy Physics
Volume 2018, Article ID 4038243, 8 pages
https://doi.org/10.1155/2018/4038243

Research Article

Analysis of Top Quark Pair Production Signal from Neutral 2HDM Higgs Bosons at LHC

Majid Hashemi and Mahbobeh Jafarpour

Physics Department, College of Sciences, Shiraz University, Shiraz 71946-84795, Iran

Correspondence should be addressed to Majid Hashemi; majid.hashemi@cern.ch

Received 12 May 2018; Revised 25 September 2018; Accepted 29 October 2018; Published 11 November 2018

Academic Editor: Burak Bilki

In this paper, the top quark pair production events are analyzed as a source of neutral Higgs bosons of the two Higgs doublet model type I at LHC. The production mechanism is $pp \longrightarrow H/A \longrightarrow t\bar{t}$ assuming a fully hadronic final state through $t \longrightarrow Wb \longrightarrow jjb$. In order to distinguish the signal from the main background which is the standard model $t\bar{t}$, we benefit from the fact that the top quarks in signal events acquire large Lorentz boost due to the heavy neutral Higgs boson. This feature leads to three collinear jets (a fat jet) which is a discriminating tool for identification of the top quarks from the Higgs boson resonances. Events with two identified top jets are selected and the invariant mass of the top pair is calculated for both signal and background. It is shown that the low $\tan\beta$ region has still some parts which can be covered by this analysis and has not yet been excluded by flavor physics data.

1. Introduction

The standard model (SM) of particle physics has taken a major step forward by observing the Higgs boson at LHC [1, 2] based on a theoretical framework known as the Higgs mechanism [3–8]. The observed particle may belong to a single SU(2) doublet (SM) or a two Higgs doublet model (2HDM) [9–11] whose lightest Higgs boson respects the observed particle properties.

One of the motivations for the two Higgs doublet model is supersymmetry where each particle has a superpartner. The supersymmetry provides an elegant solution to the gauge coupling unification, dark matter candidate, and the Higgs boson mass radiative correction by a natural parameters tuning. In such a model two Higgs doublets are required to give mass to the double space of the particles [12–14].

There are four types of 2HDMs with different scenarios of Higgs-fermion couplings. The ratio of vacuum expectation values of the two Higgs doublets ($\tan\beta = v_2/v_1$) is a measure of the Higgs-fermion coupling in all 2HDM types [15].

In general, 2HDM involves five physical Higgs bosons due to the extended degrees of freedom added to the model by introducing the second Higgs doublet. The lightest Higgs boson, h, is like the SM Higgs boson. The rest are two neutral Higgs bosons, H, A (subjects of this study), and two charged bosons, $H^{\pm}$. A review of the theory and phenomenology of 2HDM can be found in [16].

In addition to direct searches for the 2HDM Higgs bosons at colliders, there are indirect searches based on flavor physics data by investigating sources of deviations from SM when processes containing 2HDM Higgs bosons are introduced [17]. Limits obtained from these types of studies are one of the strongest limits on the mass of the charged and neutral Higgs bosons and $\tan\beta$ and will be referred to when presenting the final results.

The adopted scenario in this analysis is a search for heavy neutral Higgs boson with mass in the range 0.5-1 TeV at LHC operating at $\sqrt{s} = 14$ TeV. All heavy Higgs bosons (CP-even, CP-odd, and the charged Higgs) are assumed to be degenerate, i.e., $m_H = m_A = m_{H^{\pm}}$. The region of interest is low $\tan\beta$ and the final results will be limited to $\tan\beta < 2$. The signal process is $pp \longrightarrow H/A \longrightarrow t\bar{t} \longrightarrow W^+bW^-\bar{b} \longrightarrow jjbjjb$. The fully hadronic final state is expected to result in two fat jets (each consisting of three subjets associated with the top quark) which are examined using the updated `HEPTopTagger 2` [18, 19]. Events which contain two identified (tagged) top jets are used to fill the top pair invariant mass distribution histogram. The same approach is

Table 1: Different types of 2HDM in terms of the Higgs boson couplings with U (up-type quarks), D (down-type quarks), and L (leptons).

	Type			
	I	II	III	IV
ρ^D	$\kappa^D \cot\beta$	$-\kappa^D \tan\beta$	$-\kappa^D \tan\beta$	$\kappa^D \cot\beta$
ρ^U	$\kappa^U \cot\beta$	$\kappa^U \cot\beta$	$\kappa^U \cot\beta$	$\kappa^U \cot\beta$
ρ^L	$\kappa^L \cot\beta$	$-\kappa^L \tan\beta$	$\kappa^L \cot\beta$	$-\kappa^L \tan\beta$

applied on background events and final shape discrimination is performed to evaluate the signal significance. Before going to the details of the analysis, a brief review of the theoretical framework is presented in the next section.

2. The Higgs Sector of 2HDM

The 2HDM Lagrangian for neutral Higgs-fermion couplings as introduced in [20] takes the following form:

$$\begin{aligned}\mathscr{L}_Y = {} & \frac{1}{\sqrt{2}}\sum_f \overline{f}\left[\kappa^f s_{\beta-\alpha} + \rho^f c_{\beta-\alpha}\right] fh \\ & + \frac{1}{\sqrt{2}}\sum_f \overline{f}\left[\kappa^f c_{\beta-\alpha} - \rho^f s_{\beta-\alpha}\right] fH \\ & + \frac{i}{\sqrt{2}}\overline{f}\gamma_5\rho^f fA\end{aligned} \tag{1}$$

where h, H, A are the neutral Higgs boson fields, $\kappa^f = \sqrt{2}(m_f/v)$ for any fermion type f and $s_{\beta-\alpha} = \sin(\beta-\alpha)$, and $c_{\beta-\alpha} = \cos(\beta-\alpha)$. The ρ^f parameters define the model type and are proportional to κ^f as in Table 1 [21]. Therefore the four types of interactions (2HDM types) depend on the values of ρ^f [22].

In this study, we require $s_{\beta-\alpha} = 1$ which has two advantages. The first one is that the $s_{\beta-\alpha}$ factor in the lightest Higgs-gauge coupling is set to unity while the heavier Higgs, H, decouples from gauge bosons [16]. On the other hand, the SM-like Higgs-fermion interactions are $\tan\beta$ independent.

According to Table 1, the type I is interesting for low $\tan\beta$ as all couplings in the neutral Higgs sector are proportional to $\cot\beta$. This feature leads to cancellation of this factor as long as Higgs boson branching ratio of decay to leptons and quarks is concerned. The mass of the fermion thus plays an important role in the decay rate, and as seen from Figures 1 and 2, the Higgs boson decay to $t\bar{t}$ dominates for all relevant Higgs boson masses and $\tan\beta$ values. The decay to a pair of gluons proceeds through a preferably top quark loop and stands as the second channel. The third channel is $H/A \longrightarrow b\bar{b}$ which has been shown to be visible at LHC [23]. The current study focuses on $H/A \longrightarrow t\bar{t}$ with branching ratio being near unity and independent of the Higgs boson mass (Figure 1) and $\tan\beta$ (Figure 2).

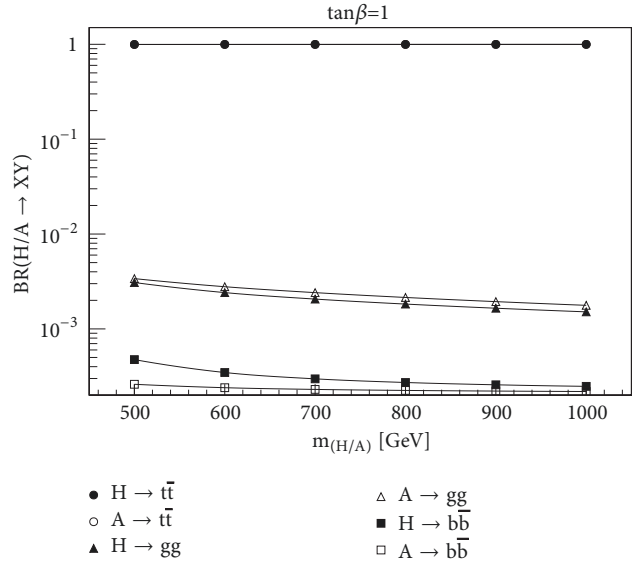

Figure 1: The branching ratio of neutral Higgs boson decays as a function of the mass. The $\tan\beta$ is set to 1.

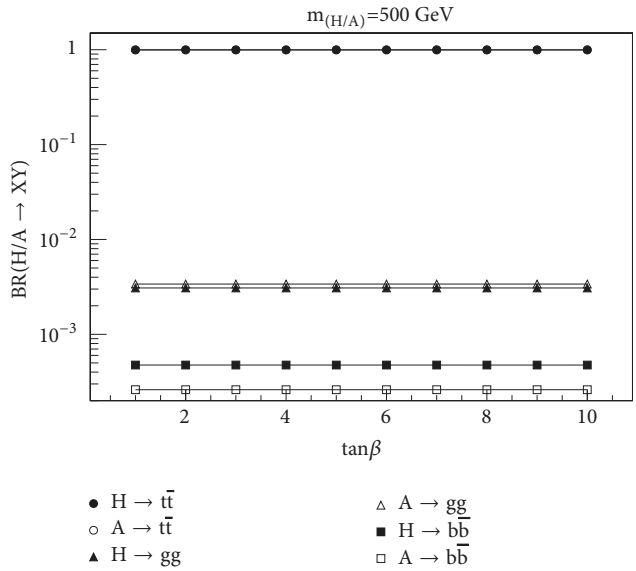

Figure 2: The branching ratio of neutral Higgs boson decays as a function of $\tan\beta$. The Higgs boson mass is set to 500 GeV.

3. Signal Identification and the Search Scenario

The signal process under study is a Higgs boson production with the Higgs boson masses in the range 500 – 1000 GeV. The three Higgs bosons masses are set to be equal for minimizing $\Delta\rho$ [24]. All selected points are checked to be consistent with the potential stability, perturbativity, and

unitarity requirements and the current experimental limits on Higgs boson masses using 2HDMC 1.6.3 [25, 26].

There has been phenomenological searches for leptophilic Higgs boson within type IV 2HDM at LHC [27] and linear colliders [28, 29]. These searches are based on leptonic decay of the Higgs boson. On the other hand, the type I 2HDM can be considered as a leptophobic model where the Higgs boson decay to quarks plays an important role. At the first glance, decays to all fermions are relevant at low tan β values. However, the fermion mass in the Higgs-fermion vertex enhances the top quark coupling dramatically compared to other channels. This is due to the fact that the common cot β factors cancel out when calculating branching ratio of Higgs decays to fermions. Therefore in this analysis, the Higgs boson decay to $t\bar{t}$ is considered as the signal.

While the neutral Higgs boson searches at LEP [30, 31] lead to $m_A \geq 93.4$ GeV, the LHC results [32, 33] indicate that the neutral Higgs boson mass in the range $m_{H/A} = 200 - 400$ GeV is excluded for tan $\beta \geq 5$. This result is based on minimal supersymmetric standard model (MSSM) which has a different Higgs boson spectrum from 2HDM due to supersymmetry constraints. Since our region of interest is Higgs boson masses above 500 GeV, no constraints from LEP or LHC limit the current analysis and the Higgs boson masses under study.

There are also results from flavor physics data. The strongest limit in this category comes from $b \longrightarrow s\gamma$ analysis which imposes lower limit on the charged Higgs mass in types II and III at 600 GeV [34–36]. There are other analyses such as $B \longrightarrow \tau\nu$, $D_s \longrightarrow \tau\nu$, $B_s \longrightarrow \mu\mu$, $B \longrightarrow K^*\gamma$, and meson mixing. Such observables have a smaller impact than $b \longrightarrow s\gamma$. All limits from the above observables as well as the one from $b \longrightarrow s\gamma$ are mainly relevant at types II and III while types I and IV are less affected due to the fact that the charged Higgs-quark coupling in processes which raise deviation from standard model is suppressed in types I and IV with increasing tan β.

In order to compare the two categories of types I/IV and II/III, one may notice that types I and IV behave differently from types II and III as far as the charged Higgs coupling to quarks is concerned. In the former, the charged Higgs coupling to all quark types is suppressed at low tan β, while, in the latter, coupling with at least one type of the quarks (up type or down type) is enhanced with tan β. Therefore charged Higgs limits from flavor physics in types I and IV are very soft and basically relevant at tan β values as low as 2. This is the region of search in this analysis. Although we are dealing with neutral Higgs bosons, since the scenario under study is a degenerate scenario based on $m_H = m_A = m_{H^\pm}$, limits on the charged Higgs are propagated into the final results.

4. Software Setup and Cross Sections

The signal cross section is obtained from PYTHIA 8.2.15 [37] using 2HDM spectrum files in LHA format [38, 39] extracted from 2HDMC 1.6.3 [25, 26]. The LHA files contain information about the parameters of the theoretical model as well as properties of any particle which may not be present in standard model, like 2HDM Higgs bosons. In this case,

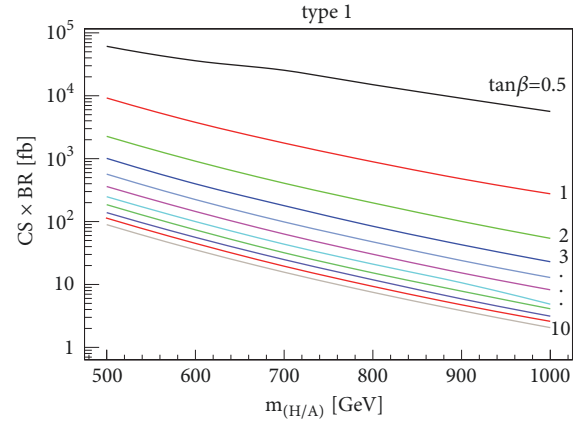

Figure 3: The signal cross section times BR($H/A \longrightarrow t\bar{t}$) at $\sqrt{s} = 14$ TeV as a function of the Higgs boson mass.

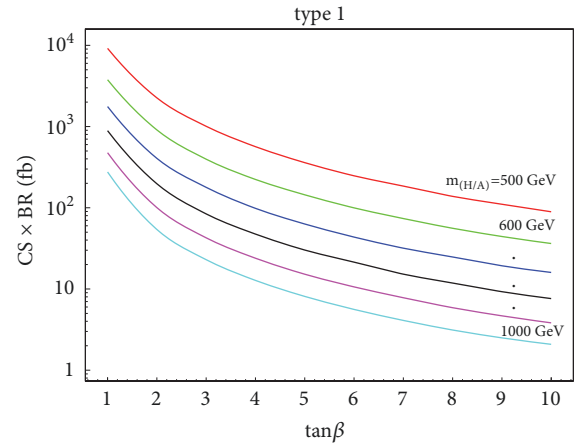

Figure 4: The signal cross section times BR($H/A \longrightarrow t\bar{t}$) at $\sqrt{s} = 14$ TeV as a function of tan β.

it contains Higgs bosons masses and their branching ratio of decays. For each benchmark point a separated LHA file is generated using 2HDMC and is passed to PYTHIA for event generation and cross section calculation. Results are shown in Figures 3 and 4 which show that the cross section decreases with increasing the Higgs boson mass as well as tan β. Therefore the most suitable area for search is where the mass is as low as possible and tan β is also very small. The main SM background processes are $t\bar{t}$, gauge boson pair production WW, WZ, ZZ, $s-$channel and $t-$channel single top, single W and single Z/γ^*, and QCD multijet events. These background processes are generated using PYTHIA except for the QCD multijet background for which Alpgen 2.14 [40–42] is used for the hard scattering generation. The output of Alpgen is stored as LHE file [38, 39] and is passed to PYTHIA for multiparticle interaction and final state showering. The cross sections are obtained using PYTHIA except for QCD samples which is obtained from Alpgen and $t\bar{t}$ for which we adopt the NLO (next to leading order) cross section calculated using MCFM [43–46]. The signal (benchmark points) and background cross sections are listed in Table 2. The QCD

Table 2: The signal and background cross sections at $\sqrt{s} = 14$ TeV. The "sts" and "stt" denote the s-channel and t-channel single top processes and QCD 6j represents QCD multijet events with 6 jets in the final state.

(a)

	Signal					
$m_{(H/A)}$ [GeV]	500	600	700	800	900	1000
$\sigma \times BR$ [fb]	61.1	36.0	25.4	15.0	9.1	5.6

(b)

	Background								
	tt	WW	WZ	ZZ	sts	stt	W	Z	QCD 6j
$\sigma \times BR$ [pb]	390	32.6	12.1	5.33	5.6	117	1.02×10^5	5.7×10^4	4×10^3

Table 3: Signal selection efficiencies and number of events at $\tan\beta = 0.5$ before the mass window cut.

	Signal					
m_H [GeV]	500	600	700	800	900	1000
eff	0.0005	0.00244	0.0055	0.0079	0.096	0.104
Events	9238	25981	41967	35703	26150	17614

multijet has a large cross section. Therefore only events with 6 jets in the final state are generated to produce the same jet multiplicity in the final state. This is based on the assumption that events with more or less number of jets do not contribute to the signal region at the end. Samples with less number of jets have a larger cross section but do not pass the selection cuts (e.g., 6 jet requirement) and those with more number of jets have much smaller cross sections and do not contribute to the signal region sizably.

5. Signal Selection and Analysis

The generation of signal and background events starts with `PYTHIA 8` [37] followed by jet reconstruction using `FASTJET 2.8` [47, 48].

The analysis uses the top tagging algorithm to identify two top jets in the final state; however, before going to that step, two selection cuts are applied to purify the signal sample. The first requirement is to have at least 2 b-jets in the final state (as there are two b-jets from the top quark decays in signal events). The b-tagging is based on a matching algorithm which uses generator level information of b quarks and compares them with reconstructed jets. If a jet is flying adjacent to a b-quark, it is considered as a b-jet with 70% probability. A 10% fake rate from c-jets is also considered as the mistagging rate.

The second requirement is a lepton veto which requires events to be free of leptons (with a transverse energy threshold of 10 GeV). This is to select fully hadronic events and reject QCD multijet events with possibility of heavy meson leptonic decays.

At this step the top tagging algorithm is applied on signal and background events. The top tagging algorithm uses a different jet reconstruction algorithm from the one used for b-tagging. The b-tagging jet algorithm is anti-kt while the top tagging algorithm is CA (Cambridge-Aachen) as discussed in what follows.

The jet reconstruction algorithms are classified according to their different subjet distance measures which can be written as $d_{j1j2} = \Delta R^2_{j1j2}/D2 \times \min(p^{2n}_{T,j1}, p^{2n}_{T,j2})$ with $n = -1, 0, 1$ for anti-k_T, Cambridge/Aachen (CA), and k_T algorithms, respectively. The k_T algorithm first combines the soft and collinear subjets and is suitable for reconstructing the QCD splitting history in top tagging algorithm. The anti-k_T algorithm, first combines the hardest subjets to obtain a stable jet with clean jet boundary. The CA algorithm always combines the most collinear subjets while not being sensitive to soft splittings and therefore is suitable for top tagging reconstruction. The algorithm adopted by `HEPTopTagger` is thus CA with a cone size of $\Delta R = 1.5$.

The `HEPTopTagger` is one of recent algorithms introduced for boosted top quark reconstruction [49]. It is based on a CA jet reconstruction with $\Delta R = 1.5$ and the top jet candidate p_T above 200 GeV. The threshold can be lowered down to 150 GeV without significant loss of efficiency [50, 51]. Having the collection of fat jets in the first step, the top tagging algorithm starts with undoing the last clustering of the top jet candidate j and requiring the mass drop criterion as $\min m_{j_i} < 0.8 m_j$ where j_i is the ith subjet from the jet j. Subjets with $m_j < 30$ GeV are not considered to end the unclustering iteration.

In the second step a filtering is applied to find a three-subjet combination with a jet mass within $m_t \pm 25$ GeV.

In the last step, having sorted jets in p_T, several requirements are applied to find the best combination of subjets with two subjets giving the best W boson invariant mass and the whole three subjets to be consistent with the top quark invariant mass. Details of these criteria are expressed in [50].

Performing the algorithm, selection efficiency for each signal sample is obtained. The same procedure is applied on background samples. Results are shown in Tables 3 and 4 for signal and background samples, respectively. These tables also include the number of events before the mass window cut. An event is required to have two top jets identified.

Table 4: Background selection efficiencies and number of events at $\tan\beta = 0.5$ before the mass window cut. The QCD sample is the 6-jet final state and STS (STT) denote the single top s-(t-) channel.

				Background					
Process	$t\bar{t}$	QCD	WW	WZ	ZZ	STS	STT	W	Z
eff	0.0027	3×10^{-5}	6×10^{-7}	2.3×10^{-6}	2.5×10^{-6}	3.8×10^{-5}	1.0×10^{-5}	0	0
Events	353525	40000	5.9	8.3	4.0	63.8	365.7	0	0

Table 5: Signal and background analysis results at $\tan\beta = 0.5$ and 1. The S and B denote the final number of signal and background events after the mass window cut.

	$m_{(H/A)}$ [GeV]					
	500	600	700	800	900	1000
Mass window [GeV]	450 – 600	530 – 620	630 – 710	710 – 820	810 – 920	870 – 1020
S	4600	16312	26915	24619	16438	12041
B	59183	63947	75728	82082	55146	52082
$\frac{S}{B}$	0.08	0.25	0.35	0.3	0.3	0.23
$\frac{S}{\sqrt{B}}$ $\tan\beta = 0.5$	18.9	64.5	97.8	85.9	70	52.8
$\frac{S}{\sqrt{B}}$ $\tan\beta = 1$	2.8	6.7	6.8	5.1	3.7	2.6

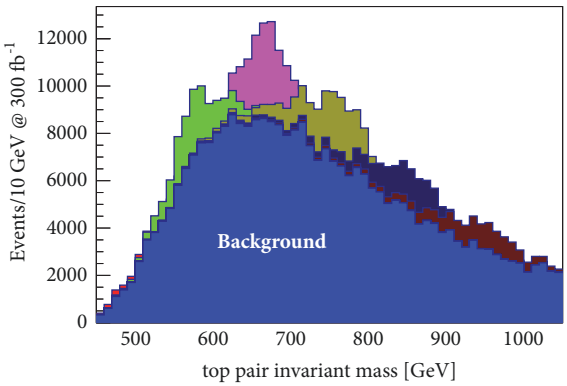

Figure 5: The signal distributions on top of the total background (shown in blue). The signal from Higgs boson masses in the range 500-1000 GeV is shown in different colors.

The invariant mass of the two top jets is calculated as the Higgs boson candidate mass. Both signal and background distributions of top quark pair invariant masses are normalized according to the corresponding cross sections. The signal on top of the background is then plotted for each benchmark point as seen in Figure 5.

The invariant mass of the top pair has a large resolution due to uncertainties in the four-momentum reconstruction of the jets as well as the top tagging algorithm. In the top tagging algorithm a χ^2 based method is used to find the correct combination of the jets with their invariant mass in agreement with the W boson and the top quark masses. There can be still ways to improve the top tagging algorithm such as normalizing the light jet four momenta to set their invariant mass equal to the W boson mass before reconstructing the top quark. Since there are two W bosons in the event, this method has some difficulties but can be studied in a detailed analysis related to the performance of the algorithm.

It should be noted that the signal distribution shown in Figure 5 has a single peak for each Higgs boson mass hypothesis due to equal masses of the Higgs bosons. Different masses hypothesis can also be considered. However, the signal distribution can not be distinguished from the equal mass scenario as long as the difference between the Higgs bosons masses is within the invariant mass resolution. Therefore scenarios with $|m_H - m_A| > 100$ GeV might be observable with two distinguishable peaks; however, such a large mass splitting raises the problem of large $\Delta\rho$ which should be avoided.

Since a large number of backgrounds fill the signal region, a mass window cut is applied to select the signal and increase the signal to background ratio. The position of the mass window (both left and right sides) is determined in an automatic search based on requiring the maximum signal significance. This is performed in a loop over bins of the histogram and finding the left and right bins inside which the signal significance is maximum.

Table 5 shows mass window position, total efficiencies for signal and background events, final number of signal and background events passing the mass window cut, their ratio, and the signal significance as $S/\sqrt{B}$ at two values of $\tan\beta = 0.5$ and 1. The integrated luminosity is set to 300 fb^{-1}. Table 5 clearly shows the high sensitivity of the signal significance to $\tan\beta$ parameter. The analysis is thus relevant to $\tan\beta$ values as low as ~ 2.

Figure 6 shows the signal significance as a function of the Higgs boson mass for different $\tan\beta$ values. The dashed horizontal line indicates the 5σ significance. As seen from

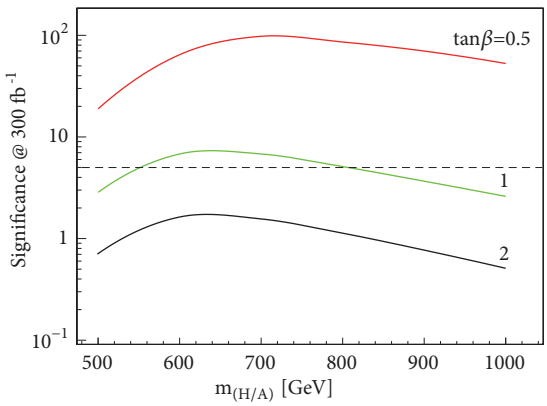

FIGURE 6: The signal significance at 300 fb^{-1} as a function of the Higgs boson mass for different values of tan β.

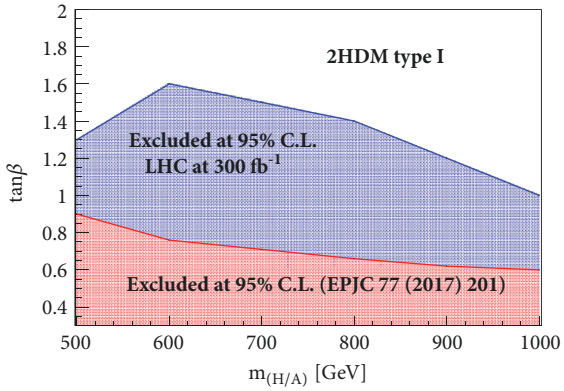

FIGURE 7: The 95% C.L. exclusion region at 300 fb^{-1}.

Figure 3 and Table 3, the signal cross section decreases with increasing Higgs boson mass while selection efficiencies increase. Therefore the product of the cross section times selection efficiency has a peak somewhere near the middle of the Higgs boson mass range where none of the cross section or selection efficiency are too small. This peak happens at m_H = 700 GeV in this analysis. Lower masses suffer from the low selection efficiency while higher masses have the problem of low cross section.

Using the analysis results for Higgs boson masses from 500 GeV to 1000 GeV, one can obtain the 95% C.L. exclusion region and the 5σ discovery contours. Figure 7 shows the exclusion region at 95% C.L. including the recent result from [35] (the result reported in [35] is based on charged Higgs mass as a function of tan β; however, it is included in the current work as a limit for all Higgs bosons since the Higgs boson masses are equal in the scenario adopted in this analysis). The 5σ contour is also shown in Figure 8.

As seen from Figures 7 and 8, both exclusion and discovery are possible at regions not yet excluded by LHC. Therefore any sign of extra top pair signals on top of SM background could be regarded as a signal for new physics especially 2HDM. It should be noted that, in this analysis, a full set of background processes was studied. However, all background processes led to very small number of events

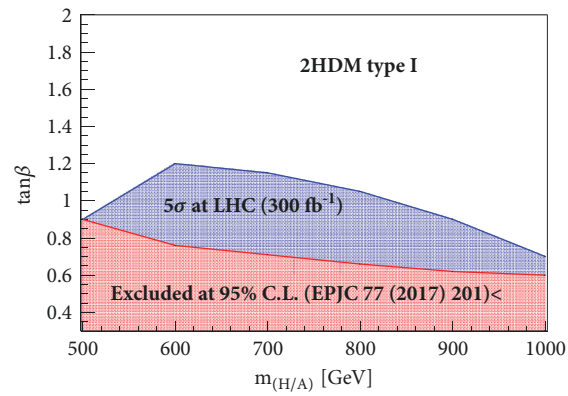

FIGURE 8: The 5σ discovery region at 300 fb^{-1}.

which were negligible compared to the SM $t\bar{t}$. Therefore final plots are based on signal on top of the $t\bar{t}$ distribution without any sizable error.

The LHC sensitivity to the signal studied in this analysis at integrated luminosity of 3000 fb^{-1} can be estimated as follows. If the signal significance grows like $\sqrt{L}$ (L is the integrated luminosity), at L = 3000 fb^{-1}, the signal significance will be roughly three times larger compared to when L = 300 fb^{-1}. The signal cross section, however, decreases from tan β = 1 to 2 by a factor of 4 as shown in Figure 4. Therefore the signal significance acquires a factor of 3/4 by increasing tan β and integrated luminosity from 1 and 300 fb^{-1} to 2 and 3000 fb^{-1}. This means that points with m_H = 600 and 700 GeV will be observable at tan β = 2 at 3000 fb^{-1}. All above considerations are of course affected by the systematic uncertainties due to the jet energy scale and four-momentum resolution as well as uncertainties in theoretical cross section calculation. A detailed analysis and estimate of such uncertainties are needed before the final assessment.

6. Discussion

The Higgs boson decay to $t\bar{t}$ is already known to dominate at 2HDM type I, and there are thorough studies of 2HDM which cover this area [52]. The aim of this work was to perform an event selection analysis based on LHC data environment and show the signal on top of the background and present exclusion contours. The scenario is taken to be a very limited case (degenerate Higgs bosons masses) to study the best possible cases (benchmark points in the parameter space). The selected benchmark points indeed lead to positive results which make the whole analysis interesting for LHC program. Furthermore, we benefit from top tagging technique which enhances the signal to background ratio and reduces the fake rate. This is in turn a test of the algorithm itself as well as benefiting from its ability in identifying the signal and reducing the background.

7. Conclusions

Extra sources of $t\bar{t}$ events from what we expect from standard model can appear from theories beyond standard model such

as two Higgs doublet models. In 2HDM type I, the heavy neutral (CP-even or odd) Higgs decay to $t\bar{t}$ dominates at low tan β. In such a scenario a proton-proton collision may create a neutral Higgs decaying to $t\bar{t}$. The signal from such a process can be observed as an excess of top pair events over what is expected from SM. The discriminating tool can be a top pair invariant mass distribution filled with events containing two top jets from both signal and background processes. The analysis performed in this work shows that such a signal is observable at integrated luminosity of 300 fb^{-1} for tan β values which depend on the Higgs boson mass. The exclusion at 95% C.L. is also possible at the same integrated luminosity for tan $\beta < 2$ with $m_{(H/A)} = 600$ GeV as the best point.

Data Availability

The data used to support the findings of this study are available from the corresponding author upon request.

Conflicts of Interest

The authors declare that they have no conflicts of interest.

Acknowledgments

This work was performed using the computing cluster at college of sciences, Shiraz University. We would like to appreciate the personnel involved in the operation and maintenance of the cluster.

References

[1] S. Chatrchyan, V. Khachatryan, A. M. Sirunyan et al., "Observation of a new boson at a mass of 125 GeV with the CMS experiment at the LHC," *Physics Letters B*, vol. 716, p. 30, 2012.

[2] ATLAS Collaboration, G. Aad, T. Abajyan, B. Abbott et al., "Observation of a new particle in the search for the Standard Model Higgs boson with the ATLAS detector at the LHC," *Physics Letters B*, vol. 716, p. 1, 2012.

[3] F. Englert and R. Brout, "Broken symmetry and the mass of gauge vector mesons," *Physical Review Letters*, vol. 13, no. 9, p. 321, 1964.

[4] P. W. Higgs, "Broken symmetries and the masses of gauge bosons," *Physical Review Letters*, vol. 13, pp. 508-509, 1964.

[5] P. Higgs, "Broken symmetries, massless particles and gauge fields," *Physics Letters*, vol. 12, no. 2, pp. 132-133, 1964.

[6] G. S. Guralnik, C. R. Hagen, and T. W. B. Kibble, "Global Conservation Laws and Massless Particles," *Physical Review Letters*, vol. 13, p. 585, 1964.

[7] P. W. Higgs, "Spontaneous symmetry breakdown without massless bosons," *Physical Review A: Atomic, Molecular and Optical Physics*, vol. 145, no. 4, pp. 1156–1163, 1966.

[8] T. W. B. Kibble, "Symmetry breaking in n-Abelian gauge theories," *Physical Review A: Atomic, Molecular and Optical Physics*, vol. 155, no. 5, pp. 1554–1561, 1967.

[9] T. D. Lee, "A Theory of Spontaneous *T* Violation," *Physical Review D: Particles, Fields, Gravitation and Cosmology*, vol. D8, p. 1226, 1973.

[10] S. L. Glashow and S. Weinberg, "Natural conservation laws for neutral currents," *Physical Review D: Particles, Fields, Gravitation and Cosmology*, vol. 15, no. 7, pp. 1958–1965, 1977.

[11] G. C. Branco, " Spontaneous ," *Physical Review D: Particles, Fields, Gravitation and Cosmology*, vol. 22, no. 11, pp. 2901–2905, 1980.

[12] I. J. R. Aitchison, "Supersymmetry and the MSSM: An Elementary Introduction," https://arxiv.org/abs/hep-ph/0505105.

[13] E. Ma and D. Ng, "New supersymmetric option for two Higgs doublets," *Physical Review D*, vol. D49, p. 6164, 1994.

[14] A. Djouadi, "The anatomy of electroweak symmetry breaking Tome II: The Higgs bosons in the Minimal Supersymmetric Model," *Physics Reports*, vol. 459, Article ID 0503173, p. 1, 1016.

[15] H. E. Haber and D. O'Neil, "Erratum: Basis-independent methods for the two-Higgs-doublet model. II. The significance of tanβ," *Physical Review D: Particles, Fields, Gravitation and Cosmology*, vol. 74, p. 059905, 2006.

[16] G. C. Branco, P. M. Ferreira, L. Lavoura, M. N. Rebelo, M. Sher, and J. P. Silva, "Theory and phenomenology of two-Higgs-doublet models," *Physics Reports*, vol. 516, p. 1, 2012.

[17] F. Mahmoudi and O. Stal, "Flavor constraints on two-Higgs-doublet models with general diagonal Yukawa couplings," *Physical Review D*, vol. 81, Article ID 035016, p. 035016, 1103, arXiv:0907.1791.

[18] T. Plehn, M. Spannowsky, M. Takeuchi, and D. Zerwas, "Stop reconstruction with tagged tops," *Journal of High Energy Physics*, vol. 2010, p. 078, 2010.

[19] T. Plehn, M. Spannowsky, and M. Takeuchi, "How to improve top-quark tagging," *Physical Review D: Particles, Fields, Gravitation and Cosmology*, vol. 85, p. 034029, 2012.

[20] S. Davidson and H. E. Haber, "Erratum: Basis-independent methods for the two-Higgs-doublet model," *Physical Review D: Particles, Fields, Gravitation and Cosmology*, vol. 72, no. 9, p. 035004, 2005.

[21] V. Barger, J. L. Hewett, and R. J. Phillips, "New constraints on the charged Higgs sector in two-Higgs-doublet models," *Physical Review D: Particles, Fields, Gravitation and Cosmology*, vol. 41, no. 11, pp. 3421–3441, 1990.

[22] M. Aoki, S. Kanemura, K. Tsumura, and K. Yagyu, "Models of Yukawa interaction in the two Higgs doublet model, and their collider phenomenology," *Physical Review D: Particles, Fields, Gravitation and Cosmology*, vol. 80, p. 015017, 2009.

[23] G. C. Dorsch, S. J. Huber, K. Mimasu, and J. M. No, "Echoes of the Electroweak Phase Transition: Discovering a Second Higgs Doublet through $A_0 \longrightarrow ZH_0$," *Physical Review Letters*, vol. 113, p. 211802, 2014.

[24] W. Grimus, L. Lavoura, O. M. Ogreid, and P. Osland, "A precision constraint on multi-Higgs-doublet models," *Journal of Physics G: Nuclear and Particle Physics*, vol. 35, no. 7, p. 075001, 2008.

[25] D. Eriksson, J. Rathsman, and O. Stal, "2HDMC – two-Higgs-doublet model calculator," *Computer Physics Communications*, vol. 181, no. 1, pp. 189–205, 2010.

[26] D. Eriksson, J. Rathsman, and O. Stal, "2HDMC — two-Higgs-doublet model calculator," *Computer Physics Communications*, vol. 181, 833, no. 4, p. 834, 2010.

[27] S. Su and B. Thomas, "The LHC Discovery Potential of a Leptophilic Higgs," *Physical Review D*, vol. 79, p. 095014, 2009.

[28] M. Hashemi, "Final state interactions in $K \longrightarrow \pi\pi$ decays: ΔI=1/2 rule vs. ε'/ε," *The European Physical Journal C*, vol. 77, p. 302, 2017.

[29] M. Hashemi and G. Haghighat, "Search for heavy neutral CP-even Higgs within lepton-specific 2HDM at a future linear collider," *Physics Letters B*, vol. 772, p. 426, 1016.

[30] R. Barate, D. Decamp, P. Ghez et al., "Search for charged Higgs bosons in e+e- collisions at energies up to sqrt(s) = 189GeV," *Physics Letters B*, vol. 487, pp. 253–263, 2000.

[31] M. Acciarri, P. Achard, O. Adrian et al., "Search for Charged Higgs Bosons in e+e- Collisions at Centre-of-Mass Energies up to 202 GeV," *Physics Letters B*, vol. 496, no. 1–2, pp. 34–42, 2000.

[32] The CMS Collaboration, A. M. Sirunyan, A. Tumasyan et al., "Search for additional neutral MSSM Higgs bosons in the $\tau\tau$ final state in proton-proton collisions at $\sqrt{s} = 13$ TeV," *Journal of High Energy Physics*, vol. 09, p. 7, 2018.

[33] M. Aaboud, G. Aad, B. Abbott et al., "Search for minimal supersymmetric standard model Higgs Bosons *H/A* and for a $Z^{'}$ boson in the $\tau\tau$ final state produced in *pp* collisions at $\sqrt{s} =$ 13 TeV with the ATLAS detector," *The European Physical Journal C*, vol. C76, no. 11, p. 585, 2016.

[34] M. Misiak, H. M. Asatrian, R. Boughezal et al., "Updated NNLO QCD predictions for the weak radiative B-meson decays," *Physical Review Letters*, vol. 114, Article ID 221801, p. 221801, 2015.

[35] M. Misiak and M. Steinhauser, "Weak radiative decays of the B meson and bounds on $M_{H}\pm$ in the Two-Higgs-Doublet Model," *The European Physical Journal C*, vol. 77, p. 201, 2017.

[36] A. Arbey, F. Mahmoudi, O. Stal, and T. Stefaniak, "Status of the Charged Higgs Boson in Two Higgs Doublet Models," *The European Physical Journal C*, vol. 78, p. 182, 2018.

[37] T. Sjostrand, S. Mrenna, and P. Z. Skands, "A brief introduction to PYTHIA 8.1," *Computer Physics Communications*, vol. 178, no. 11, pp. 852–867, 1016.

[38] J. Alwall, A. Ballestrero, P. Bartalini et al., "Monte Carlos for the LHC," in *Proceedings of the Workshop on the Tools for LHC Event Simulation (MC4LHC)*, Geneva, Switzerland, July, 2006.

[39] J. Alwall, A. Ballestrero, P. Bartalini et al., "A standard format for Les Houches Event Files," *Computer Physics Communications*, vol. 176, no. 4, pp. 300–304, 2007.

[40] F. Caravaglios, M. L. Mangano, M. Moretti, and R. Pittau, "A new approach to multi-jet calculations in hadron collisions," *Nuclear Physics B*, vol. 539, no. 1-2, pp. 215–232, 1999.

[41] M. L. Mangano, M. Moretti, and R. Pittau, "Multijet matrix elements and shower evolution in hadronic collisions: Wbb̄+n-jets as a case study," *Nuclear Physics B*, vol. 632, pp. 343–362, 2002.

[42] M. L. Mangano, F. Piccinini, A. D. Polosa, M. Moretti, and R. Pittau, "ALPGEN, a generator for hard multiparton processes in hadronic collisions," *Journal of High Energy Physics*, vol. 2003, no. 07, p. 001, 2003.

[43] J. M. Campbell, R. K. Ellis, and F. Tramontano, "Single top production and decay at next-to-leading order," *Physical Review D*, vol. D70, p. 094012, 2004.

[44] J. M. Campbell and F. Tramontano, "Next-to-leading order corrections to Wt production and decay," *Nuclear Physics B*, vol. 726, p. 109, 2005.

[45] J. M. Campbell, R. Frederix, F. Maltoni, and F. Tramontano, "Next-to-Leading-Order Predictions for," *Physical Review Letters*, vol. 102, p. 182003, 2009.

[46] J. M. Campbell and R. K. Ellis, "Top-quark processes at NLO in production and decay," https://arxiv.org/abs/1204.1513.

[47] M. Cacciari, "FastJet: a code for fast k_t clustering, and more," in *Proceedings of the 14th International Workshop, DIS*, Tsukuba, Japan, https://arxiv.org/abs/hep-ph/0607071.

[48] M. Cacciari, G. P. Salam, and G. Soyez, "FastJet user manual: (For version 3.0.2)," *The European Physical Journal C*, vol. 72, no. 3, article 1896, pp. 1–54, 2012.

[49] T. Plehn and M. Spannowsky, "Top Tagging," *Journal of Physics G: Nuclear and Particle Physics*, vol. G39, p. 083001, 2012.

[50] S. Yang and Q.-S. Yan, "Searching for Heavy Charged Higgs Boson with Jet Substructure at the LHC," *Journal of High Energy Physics*, vol. 02, p. 074, 2012.

[51] M. Hashemi and G. Haghighat, "Observability of s-channel Heavy Charged Higgs at LHC Using Top Tagging Technique," *Journal of High Energy Physics*, vol. 02, p. 040, 2016.

[52] B. Dumont, J. F. Gunion, Y. Jiang, and S. Kraml, "Constraints on and future prospects for Two-Higgs-Doublet Models in light of the LHC Higgs signal," *Physical Review D*, vol. D90, p. 035021, 2014.